

## Conductance-Based Integrate-and-Fire Models

**Alain Destexhe**

*Department of Physiology, Laval University School of Medicine,  
Québec, G1K 7P4, Canada*

**A conductance-based model of  $\text{Na}^+$  and  $\text{K}^+$  currents underlying action potential generation is introduced by simplifying the quantitative model of Hodgkin and Huxley (HH). If the time course of rate constants can be approximated by a pulse, HH equations can be solved analytically. Pulse-based (PB) models generate action potentials very similar to the HH model but are computationally faster. Unlike the classical integrate-and-fire (IAF) approach, they take into account the changes of conductances during and after the spike, which have a determinant influence in shaping neuronal responses. Similarities and differences among PB, IAF, and HH models are illustrated for three cases: high-frequency repetitive firing, spike timing following random synaptic inputs, and network behavior in the presence of intrinsic currents.**

### 1 Introduction ---

Over 40 years ago, Hodgkin and Huxley introduced a remarkably successful quantitative description of action potentials (Hodgkin & Huxley, 1952). More recent techniques revealed that transmembrane ionophores underlie ionic currents and that the assumptions of the Hodgkin-Huxley (HH) model were essentially correct if reinterpreted in the light of current knowledge on the activation of ion channels (see Hille, 1992). Although Markov kinetic models describe the properties of sodium channels more adequately (Vandenberg & Bezanilla, 1991), the success of the HH model is due to its “observability,” as its parameters are easily evaluated from voltage-clamp experiments. It remains the most widely used description of voltage-dependent conductances.

The drawback of using HH models is that they require solving a set of several first-order differential equations in addition to cable equations. Moreover, numerical integration of these equations can require relatively small integration steps due to the nonlinearity and fast kinetics of the  $\text{Na}^+$  and  $\text{K}^+$  currents underlying action potentials. This fine integration is then imposed to the whole system, which may have slower currents that would not require such a high temporal resolution but may result in needs of considerable computation time for simulating large-scale neuronal networks.

An alternative approach was to simplify the process of action potential generation by representing the neuron as an integrate-and-fire (IAF) device (see Arbib, 1995). In this case, the neuron produces a spike when its membrane potential crosses a given threshold value and the membrane is instantaneously reset to its resting level. Although this type of model has been extensively used for representing large-scale neuronal networks, an important drawback is that it neglects the variations of  $\text{Na}^+$  and  $\text{K}^+$  conductances, which may have important effects in spike generation (Mainen, 1995). Moreover, central neurons have been shown to contain a large spectrum of other intrinsic currents, which have a determinant effect on firing behavior (Llinás, 1988). In this case, the IAF paradigm is clearly inappropriate.

In this article, we propose a simplified model of action potentials based on HH equations. Besides its similarity with IAF models, this method is shown to capture the conductance changes due to action potentials, which has a determinant influence on electrophysiological behavior.

## 2 Pulse-Based Models for Voltage-Dependent Currents

---

We start from the equations of Hodgkin and Huxley (1952):

$$\begin{aligned} C_m \dot{V} &= -g_{\text{leak}} (V - E_{\text{leak}}) - \bar{g}_{\text{Na}} m^3 h (V - E_{\text{Na}}) - \bar{g}_{\text{Kd}} n^4 (V - E_{\text{K}}) \\ \dot{m} &= \alpha_m(V) (1 - m) - \beta_m(V) m \\ \dot{h} &= \alpha_h(V) (1 - h) - \beta_h(V) h \\ \dot{n} &= \alpha_n(V) (1 - n) - \beta_n(V) n \end{aligned} \quad (2.1)$$

where  $V$  is the membrane potential,  $C_m = 1 \mu\text{F}/\text{cm}^2$  is the membrane capacitance, and  $g_{\text{leak}} = 0.1 \text{ mS}/\text{cm}^2$  and  $E_{\text{leak}} = -70 \text{ mV}$  are the leak conductance and reversal potential, respectively.  $\bar{g}_{\text{Na}} = 100 \text{ mS}/\text{cm}^2$  and  $\bar{g}_{\text{Kd}} = 80 \text{ mS}/\text{cm}^2$  are the maximal conductances of the sodium current and delayed rectifier with reversal potentials of  $E_{\text{Na}} = 50 \text{ mV}$  and  $E_{\text{K}} = -90 \text{ mV}$ .  $m$ ,  $h$ , and  $n$  are the activation variables, whose time evolution depends on the voltage-dependent rate constants  $\alpha_m$ ,  $\beta_m$ ,  $\alpha_h$ ,  $\beta_h$ ,  $\alpha_n$ , and  $\beta_n$ . The voltage-dependent expressions of the rate constants were as in the version described by Traub and Miles (1991).

The behavior of the HH model in a single compartment cell during a train of action potentials is shown in Figure 1 (left panel). As a consequence of the rapid changes in membrane voltage during action potentials, the time course of the rate constants exhibits sharp transitions. This is best illustrated by the behavior of  $\alpha_m$ : the function  $\alpha_m(V)$  is approximately zero for the whole range of membrane potential below  $\sim -50 \text{ mV}$ , then increases progressively with depolarization; consequently, before and after the action potential,  $\alpha_m \sim 0$  and has positive values only during the spike (see Fig. 1).

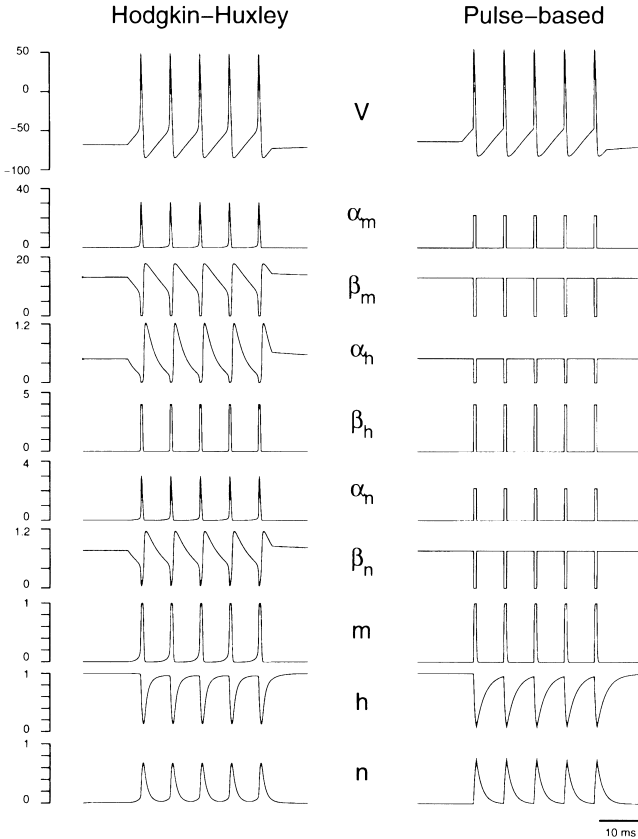


Figure 1: Comparison of action potential generation in Hodgkin-Huxley and pulse-based models. A train of spikes was generated by injecting a depolarizing current pulse (2 nA) in a single compartment model (area of  $15,000 \mu\text{m}^2$ ;  $\bar{g}_{Kd} = 30 \text{ ms/cm}^2$ ; other parameters as in equation 2.1). The time course of the rate constants ( $\alpha_m$ ,  $\beta_m$ ,  $\alpha_h$ ,  $\beta_h$ ,  $\alpha_n$ , and  $\beta_n$ ) and state variables ( $m$ ,  $h$ , and  $n$ ) is shown for each panel. In the Hodgkin-Huxley model (left panel), rate constants undergo sharp transitions when a spike occurs. Approximating these transitions by pulses (right panel) led to a simplified representation of spike-generating mechanisms (threshold of  $-53 \text{ mV}$ , pulse duration of  $0.6 \text{ ms}$ , rate values as in equation 4).

The basis of the simplified model is to approximate the time course of the rate constants by a pulse triggered when the membrane potential crosses a

given threshold. For example,  $\alpha_m$  will be assigned a positive value during the pulse and will be zero otherwise. Generalizing for other rate constants, before and after the pulse, we have:

$$\begin{aligned}\alpha_m &= 0, & \beta_m &= \beta_M \\ \alpha_h &= \alpha_H, & \beta_h &= 0 \\ \alpha_n &= 0, & \beta_n &= \beta_N\end{aligned}\quad (2.2)$$

whereas during the pulse:

$$\begin{aligned}\alpha_m &= \alpha_M, & \beta_m &= 0 \\ \alpha_h &= 0, & \beta_h &= \beta_H \\ \alpha_n &= \alpha_N, & \beta_n &= 0.\end{aligned}\quad (2.3)$$

Here,  $\alpha_M$ ,  $\beta_M$ ,  $\alpha_H$ ,  $\beta_H$ ,  $\alpha_N$ , and  $\beta_N$  are constant values. They are estimated from the value of the voltage-dependent expressions at hyperpolarized and depolarized potentials. Choosing  $-70$  mV and  $+20$  mV and using Traub and Miles's formulation gives:

$$\begin{aligned}\alpha_M &= \alpha_m(20) \simeq 22 \text{ ms}^{-1} \\ \beta_M &= \beta_m(-70) \simeq 13 \text{ ms}^{-1} \\ \alpha_H &= \alpha_h(-70) \simeq 0.5 \text{ ms}^{-1} \\ \beta_H &= \beta_h(20) \simeq 4 \text{ ms}^{-1} \\ \alpha_N &= \alpha_n(20) \simeq 2.2 \text{ ms}^{-1} \\ \beta_N &= \beta_n(-70) \simeq 0.76 \text{ ms}^{-1}.\end{aligned}\quad (2.4)$$

It is then straightforward to solve equations 2.1, leading to the following expressions: before and after the pulse, the rate constants are given by:

$$\begin{aligned}m(t) &= m_0 \exp[-\beta_M(t - t_0)] \\ h(t) &= 1 + (h_0 - 1) \exp[-\alpha_H(t - t_0)] \\ n(t) &= n_0 \exp[-\beta_N(t - t_0)]\end{aligned}\quad (2.5)$$

where  $t_0$  is the time at which the last pulse ended, and  $m_0$ ,  $h_0$ , and  $n_0$  are the values of  $m$ ,  $h$ , and  $n$  at that time.

During the pulse, the rate constants are given by:

$$\begin{aligned}m(t) &= 1 + (m_0 - 1) \exp[-\alpha_M(t - t_0)] \\ h(t) &= h_0 \exp[-\beta_H(t - t_0)] \\ n(t) &= 1 + (n_0 - 1) \exp[-\alpha_N(t - t_0)].\end{aligned}\quad (2.6)$$

Here,  $t_0$  is the time at which the pulse began, and  $m_0$ ,  $h_0$ , and  $n_0$  are the values of  $m$ ,  $h$ , and  $n$  at that time.

Using this procedure, the simplified model generated action potentials similar to the HH model (see Fig. 1, right panel). The time course of the activation variables  $m$ ,  $h$ , and  $n$  was also comparable in both models. The optimal values of parameters were estimated by fitting expressions 2.5 and 2.6 directly to the original HH model. Using a simplex procedure (Press et al., 1986), and starting from different initial values of the parameters, the fitting led to a unique estimate of the pulse duration ( $0.6 \pm 0.08$  ms) and of the membrane threshold ( $-50.1 \pm 0.3$  mV; other parameters were as in Fig. 1).

The computational efficiency of the pulse-based mechanism is essentially due to the direct estimation of variables  $m, h, n$  from the membrane potential (see equations 2.5 and 2.6). Another factor providing further acceleration is that outside the pulse, an expression similar to equation 2.5 can be written for  $m^3$  and  $n^4$ , which greatly reduces the number of multiplications since no exponentiation is calculated.

### 3 Comparison of Pulse-Based Models with Other Mechanisms

The important point of pulse-based (PB) models is that they provide a good approximation of dynamical properties of firing behavior described by the HH mechanism. These properties were tested in three ways: repetitive firing, random firing, and network behavior. First, the optimized PB model was compared to HH and IAF mechanisms following injection of current pulses of increasing amplitudes (see Fig. 2). Pulse-based models gave an excellent approximation of interspike intervals at different firing frequencies, the spike shape, and the rise and decay of the membrane potential. On the other hand, the IAF model taken in the same conditions gave a poor approximation (see Fig. 2). For IAF models, the threshold or the absolute refractory period affected the frequency of firing, but variations of these parameters failed to generate the correct firing frequencies.

Second, PB models were tested in the case of random synaptic bombardment in a single-compartment cell having AMPA and GABA<sub>A</sub> postsynaptic receptors (see Fig. 3). The conductance of synaptic currents was chosen such that most postsynaptic potentials were subthreshold, occasionally leading to firing. This subthreshold dynamics is surprisingly irrelevant for spiking as PB and IAF mechanisms behaved very closely to the HH model (see Fig. 3), with spike timing differences of  $1.1 \pm 1.8$  ms (average  $\pm$  standard deviation) and rare occurrences of nonmatching spikes. The precision in spike timing was very sensitive to the value of the threshold and slightly better for PB models.

Third, PB models were tested in network simulations having both intrinsic and synaptic currents, besides  $I_{Na}$  and  $I_{Kd}$ . The network considered was a model of spindle oscillations in interconnected thalamocortical (TC) and

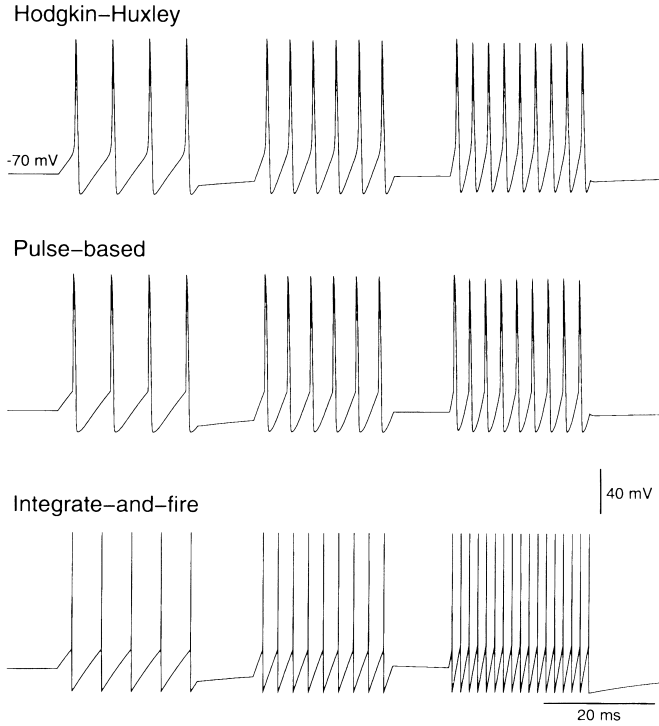


Figure 2: Comparison of repetitive firing with three different models. A single compartment cell (same parameters as in equation 1) was simulated with injection of three depolarizing current pulses of increasing amplitudes (1 nA, 2 nA, and 4 nA). Top trace: Simulation using the original Hodgkin-Huxley model. Middle trace: Simulation using pulse-based equations (identical parameters as in Figure 1, right). Bottom trace: Simple integrate-and-fire model (the spike consisted of a sudden rise to 50 mV, immediately followed by a reset to  $-90$  mV and an absolute refractory period of 1.5 ms; same threshold as the pulse-based mechanism). All models had identical passive properties.

thalamic reticular (RE) neurons (Destexhe, Bal, McCormick, & Sejnowski, 1996). These neurons have a set of intrinsic sodium, potassium, calcium, and cationic currents, allowing the cell to produce different types of bursts of action potentials (see Steriade, McCormick, & Sejnowski, 1993). Although single TC and RE cells do not necessarily generate sustained oscillations, interconnected TC and RE cells with excitatory (AMPA-mediated) and inhibitory (GABAergic) synapses can display spindle oscillations, as seen from

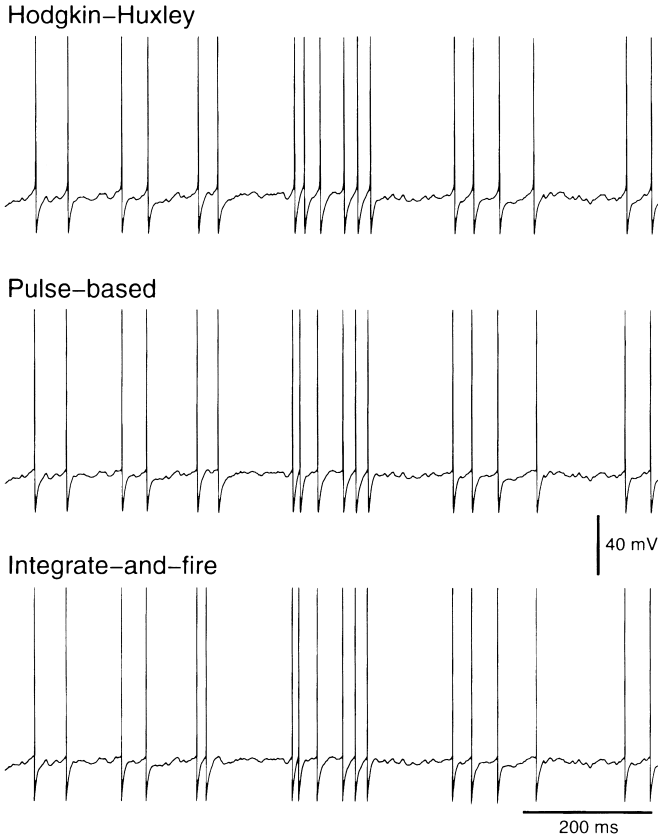


Figure 3: Comparison of pulse-based and original Hodgkin-Huxley models using random synaptic bombardment. Top panel: Single compartment model (same parameters as in equation 1) with 100 excitatory (AMPA-mediated) and 10 inhibitory ( $GABA_A$ -mediated) synaptic inputs. Synaptic currents were described by kinetic models (Destexhe et al., 1997) and had maximal conductances of 1.5 and 6 nS for each simulated AMPA- and  $GABA_A$ -mediated contact, respectively. Each synaptic input was random (Poisson distributed) with a mean rate of 50 Hz. Middle panel: Same simulation with action potentials generated using pulse-based models. Bottom panel: Same simulation using integrate-and-fire mechanisms.

in vivo and in vitro recordings (Steriade et al., 1993). This behavior was successfully reproduced by the model using either HH equations or PB models (see Fig. 4). As in the case of synaptic bombardment, action potential timing

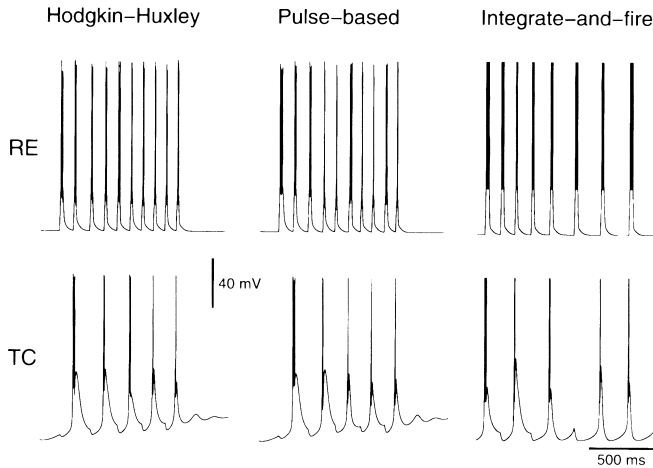


Figure 4: Comparison of simplified and original Hodgkin-Huxley models using simulations of circuits of neurons. Left panel: Model of spindle oscillations in a network of 16 thalamic neurons. Eight thalamocortical (TC) cells projected to 8 thalamic reticular (RE) neurons using AMPA-mediated contacts, whereas RE cells contacted themselves using  $GABA_A$  receptors and TC cells using a mixture of  $GABA_A$  and  $GABA_B$  receptors. Each neuron had  $Na^+$ ,  $K^+$ ,  $Ca^+$ , and cationic voltage-dependent currents described by Hodgkin-Huxley-type equations, whose parameters were obtained from voltage-clamp and current-clamp data (Destexhe et al., 1996). One cell of each type is represented during a spindle sequence. Middle panel: Same simulation using pulse-based mechanisms for action potentials. Right panel: Same simulation using integrate-and-fire models.

was not rigorously identical in the two models, but spindle oscillations had the correct frequency and phase relationships between cells. On the other hand, the high-frequency firing of TC and RE cells was not well captured by IAF mechanisms, which gave rise to different oscillation frequencies at the network level (see the right panel of Fig. 4).

Finally, the computational performance was compared for different mechanisms of spike generation in a single compartment cell. Table 1 shows that the PB method is significantly faster than differential equations (DE). According to the algorithms available with the NEURON simulator (Hines, 1993), the integration of HH equations can be optimized (DEo) by using precalculated rate constants, tabulated as a function of  $V$ . Although these optimized HH equations led to substantial acceleration (DEo vs. DE), they were not as efficient as PB models, which estimate  $m$ ,  $h$ , and  $n$  directly from  $V$ . Simple IAF models showed the highest performance.

Table 1: Computational Performance of Different Methods for Generating Action Potentials.

Method	NEURON (relative CPU time)	Minimal C Code (relative CPU time)
DE	1	1
DEo	0.32	0.45
PB	0.25	0.17
IAF	0.23 <sup>a</sup>	0.08

Note: A single-compartment cell comprising passive currents, 1 nA injected current, and a model for action potentials was simulated. Different models for action potentials were: DE: Hodgkin-Huxley model described by differential equations; DEo: same equations solved using optimized algorithms; PB: pulse-based model; IAF: simple integrate-and-fire model. A backward Euler integration scheme was used with a time step of 0.025 ms over a total simulated time of 50 seconds. The equations were solved using either the NEURON simulator (Hines, 1993) or directly in C code (minimal code for solving the equations without graphic interface; the exact same algorithms and optimizations as in NEURON were used). Codes are available on request.

<sup>a</sup> IAF models could not be implemented optimally in NEURON.

## 4 Discussion

This article has presented a novel method to approximate the dynamics of action potentials. The model was based on the HH equations in which the time course of rate constants was approximated by a short pulse. In a previous article (Destexhe, Mainen, & Sejnowski, 1994a), similar PB mechanisms were introduced to model synaptic currents. The basis of the synaptic model was that artificially applied pulses of agonist gave rise to postsynaptic currents with a time course very similar to the intact synapse (e.g., Colquhoun, Jonas, & Sakmann, 1992). PB models of synaptic currents offered the advantages of being simple and fast, and they could be easily fit to experimental data.

In the case reported in this article, the pulse approximation of HH equations was based on the observation that rate constants undergo sharp transitions during action potentials (see Fig. 1), also leading to analytic resolution and therefore fast algorithms that can be fit easily to any template. In principle, the same approximation could be considered for other types of channels, under the important condition that rate constants display sharp transitions. A possible example would be Ca<sup>2+</sup>-dependent channels, assuming that an action potential triggers a short pulse of intracellular Ca<sup>2+</sup> concentration due to high-threshold Ca<sup>2+</sup> currents.

Are PB models different from conventional IAF mechanisms? Both methods share a fixed voltage threshold as well as a dead time following spikes to represent the absolute refractory period. PB models, however, significantly

differ from IAF models because they take into account the decay of variables  $m$ ,  $h$ , and  $n$  in between spikes, which has a determinant influence on repetitive firing at high frequencies. In IAF models, the membrane is reset instantaneously after a spike to a hyperpolarized level. In PB models, the reset occurs through the activation of the delayed-rectifier current, which has an effect over a longer period of time due to the relatively slow decay of the variable  $n$ . This is the main factor that affected the frequency of firing in Figure 2. However, we cannot exclude the possibility that more sophisticated IAF models (with relative refractory period or variable threshold) would reproduce these properties, although it still remains to be demonstrated.

Are PB models different from precalculated conductance waveforms? The model presented here is more sophisticated than simply pasting a conductance waveform, as the changes in variables  $m$ ,  $h$ , and  $n$  depend on their initial values at the time of the spike. Conductance changes are different during low- and high-frequency firing, and PB models propose simplified equations to capture these changes. This is similar to comparing alpha functions with PB models of synaptic currents: Alpha functions do not provide correct postsynaptic summation, whereas it is well captured by PB models (see Destexhe, Mainen, & Sejnowski, 1994b).

When do PB models fail? It was shown here that PB models approximate well HH equations for high-frequency firing during injection of current pulses (see Fig. 2), following random synaptic inputs (see Fig. 3), or in network simulations where intrinsic and synaptic currents were present (see Fig. 4). However, as the spike is defined from a fixed threshold, PB models would not apply to cases with significant subthreshold contribution of the HH mechanism in determining spike timing or if there are dynamical changes in the threshold. PB models cannot be applied to model various properties of sodium channels, such as the progressive spike inactivation during bursting, anode-break excitation, voltage-dependent recovery from inactivation, and more generally the response of these channels during voltage-clamp experiments. In these cases, spike generation should be modeled with the original HH equations or a more accurate mechanism.

How do PB models compare to other types of simplifications of HH equations? Several models were proposed to reduce HH equations to fewer variables (e.g., Fidzhugh, 1961; Krinskii & Kokoz, 1973; Hindmarsh & Rose, 1982; Rinzel, 1985; Kepler, Abbott, & Marder, 1992). Another type of simplification was to start from detailed kinetic models for the gating of  $\text{Na}^+$  or  $\text{K}^+$  channels and then simplify this scheme until reaching the minimal number of states to account for the behavior of the current (Destexhe et al., 1994b). Pulse-based models are different from these previous approaches; the simplifying assumptions of these models lead to a complete analytical resolution of HH equations, and therefore no differential equation must be solved (see also Miller, 1979).

How large is the increase of computational efficiency? PB models provide a substantial acceleration compared to HH equations, approaching the per-

formance of IAF models (see Table 1). However, this increase of efficiency could be minimal in the case of network simulations where action potentials represent only a small fraction of the computation time. On the other hand, if PB models could be used in conjunction with pulse-based mechanisms applied to other types of currents, such as synaptic currents (Destexhe et al., 1994a; Lytton, 1996), then this approach could provide a considerable acceleration of computation time.

How can PB models be improved? An obvious improvement would be to apply the PB approximation to a simplified model of action potentials, such as that of Hindmarsh and Rose (1982), leading to PB models with fewer variables. Another improvement would be to add a relative refractory period or a variable threshold, for example, by making the threshold depend on the value of the inactivation variable  $h$ . More optimal values of rate constants than equation 2.4 could also be obtained by fitting the model directly to HH equations using several templates, such as that of Figs. 2 and 3.

In conclusion, PB models capture important features of the firing behavior as described by HH mechanisms, but they do not apply to all cases. This approach is intermediate between simple IAF and more detailed biophysical models and may facilitate building large-scale network simulations that incorporate the intrinsic electrophysiological properties of single cells.

## Acknowledgments

---

All simulations were run on a Sun Sparc 20 workstation using the NEURON simulator (Hines, 1993) or using programs written in C. Research was supported by MRC (Medical Research Council of Canada), and start-up funds came from FRSQ (Fonds de la Recherche en Santé du Québec).

## References

---

- Arbib, M. (1995). *The handbook of brain theory and neural networks*. Cambridge, MA: MIT Press.
- Colquhoun, D., Jonas, P., & Sakmann, B. (1992). Action of brief pulses of glutamate on AMPA/KAINATE receptors in patches from different neurons of rat hippocampal slices. *J. Physiol.*, *458*, 261–287.
- Destexhe, A., Mainen, Z., & Sejnowski, T. J. (1997). Kinetic models of synaptic transmission. In C. Koch & I. Segev, (Eds.), *Methods in Neuronal Modeling* (2nd ed.). Cambridge, MA: MIT Press.
- Destexhe, A., Bal, T., McCormick, D. A., & Sejnowski, T. J. (1996). Ionic mechanisms underlying synchronized oscillations and propagating waves in a model of ferret thalamic slices. *J. Neurophysiol.*, *76*, 2049–2070.
- Destexhe, A., Mainen, Z., & Sejnowski, T. J. (1994a). An efficient method for computing synaptic conductances based on a kinetic model of receptor binding. *Neural Computation*, *6*, 14–18.

- Destexhe, A., Mainen, Z., & Sejnowski, T. J. (1994b). Synthesis of models for excitable membranes, synaptic transmission and neuromodulation using a common kinetic formalism. *J. Computational Neurosci.*, *1*, 195–230.
- Fidzhugh, R. (1961). Impulses and physiological states in models of nerve membrane. *Biophys. J.*, *1*, 445–466.
- Hille, B. (1992). *Ionic channels of excitable membranes*. Sunderland, MA: Sinauer Associates.
- Hindmarsh, J. L., & Rose, R. M. (1982). A model of the nerve impulse using two first-order differential equations. *Nature*, *296*, 162–164.
- Hines, M. (1993). NEURON—A program for simulation of nerve equations. In F. H. Eeckman (Ed.), *Neural Systems: Analysis and Modeling* (pp. 127–136). Boston: Kluwer Academic Publishers.
- Hodgkin, A. L., & Huxley, A. F. (1952). A quantitative description of membrane current and its application to conduction and excitation in nerve. *J. Physiol. (London)*, *117*, 500–544.
- Kepler, T. B., Abbott, L. F., & Marder, E. (1992). Reduction of conductance-based neuron models. *Biol. Cybernetics*, *66*, 381–387.
- Krinskii, V. I., & Kokoz, Y. M. (1973). Analysis of the equations of excitable membranes—1. Reduction of the Hodgkin-Huxley equations to a second-order system. *Biofizika*, *18*, 506–511.
- Llinás, R. R. (1988). The intrinsic electrophysiological properties of mammalian neurons: A new insight into CNS function. *Science*, *242*, 1654–1664.
- Lytton, W. W. (1996). Optimizing synaptic conductance calculation for network simulations. *Neural Computation*, *8*, 501–509.
- Mainen, Z. F. (1995). *Mechanisms of spike generation in neocortical neurons*. Unpublished doctoral dissertation, University of California, San Diego.
- Miller, R. M. (1979). A simple model of delay, block and one way conduction in Purkinje fibers. *J. Math. Biol.*, *7*, 385–398.
- Press, W. H., Flannery, B. P., Teukolsky, S. A., & Vetterling, W. T. (1986). *Numerical recipes: The art of scientific computing*. Cambridge: Cambridge University Press.
- Rinzel, J. (1985). Excitation dynamics: Insights from simplified membrane models. *Fed. Proc.*, *44*, 2944–2946.
- Steriade, M., McCormick, D. A., & Sejnowski, T. J. (1993). Thalamocortical oscillations in the sleeping and aroused brain. *Science*, *262*, 679–685.
- Traub, R. D., & Miles, R. (1991). *Neuronal networks of the hippocampus*. Cambridge: Cambridge University Press.
- Vandenberg, C. A., & Bezanilla, F. (1991). A model of sodium channel gating based on single channel, macroscopic ionic, and gating currents in the squid giant axon. *Biophys. J.*, *60*, 1511–1533.